

# Epidemic outbreaks in complex heterogeneous networks

Yamir Moreno\*, Romualdo Pastor-Satorras<sup>†</sup> and Alessandro Vespignani\*

*\*The Abdus Salam International Centre for Theoretical Physics, P.O. Box 586, 34100 Trieste,*

*Italy*

*<sup>†</sup>Departament de Física i Enginyeria Nuclear, Universitat Politècnica de Catalunya*

*Campus Nord, Mòdul B4, 08034 Barcelona, Spain*

(October 25, 2018)

## Abstract

We present a detailed analytical and numerical study for the spreading of infections in complex population networks with acquired immunity. We show that the large connectivity fluctuations usually found in these networks strengthen considerably the incidence of epidemic outbreaks. Scale-free networks, which are characterized by diverging connectivity fluctuations, exhibit the lack of an epidemic threshold and always show a finite fraction of infected individuals. This particular weakness, observed also in models without immunity, defines a new epidemiological framework characterized by a highly heterogeneous response of the system to the introduction of infected individuals with different connectivity. The understanding of epidemics in complex networks might deliver new insights in the spread of information and diseases in biological and technological networks that often appear to be characterized by complex heterogeneous architectures.

## I. INTRODUCTION

The epidemiology of heterogeneous networks has largely benefitted from the need of understanding the spreading of human sexual diseases in the complex web of sexual partnership [1–3]. Epidemic modeling considered that population groups can be characterized in classes having different sexual activity or number of sexual contacts. This fact leads to models dealing with heterogeneous populations which are known to enhance the spread of infections as well as make them harder to eradicate (for a review see [4]). In this perspective, a limiting case is represented by the newly identified classes of complex networks (for a review see [5]). The highly heterogeneous topology of these networks is mainly reflected in the small average path lengths among any two nodes (small-world property) [6,7], and in a power law distribution (scale-free property),  $P(k) \sim k^{-2-\gamma}$ , for the probability that any node has  $k$  connections to other nodes [8]. While regular networks present finite connectivity fluctuations ( $\langle k \rangle \simeq \langle k^2 \rangle$ ), scale-free (SF) networks are a limiting case of heterogeneity where connectivity fluctuations are diverging if  $0 < \gamma \leq 1$ . In other words, the network nodes possess a statistically significant probability of having a virtually unbounded number of connections compared to the average value. SF networks find real examples in several technological networks such as the Internet [9,10] and the world-wide-web (WWW) [11], as well as in natural systems such as food-webs, and metabolic or protein networks [5]. The need to understand the dynamics of information transmission, the error tolerance [12–14] and other properties of complex networks has therefore called for the study of epidemic modeling in complex networks [15–19].

A surprising result, originated by the inspection of the susceptible-infected-susceptible (SIS) model, has shown that the spread of infections is tremendously strengthened on SF networks [18,19]. Opposite to standard models, epidemic processes in these networks do not possess any epidemic threshold below which the infection cannot produce a major epidemic outbreak or an endemic state. In principle, SF networks are prone to the persistence of diseases whatever infective rate they may have. This feature reverberates also in the choice of immunization strategies [20–22] and changes radically many standard conclusions on epidemic spreading. This study appears particularly relevant in the case of technological networks, for instance for the spreading of digital viruses in the Internet [18], and it has soon been generalized by showing that also the susceptible-infected-removed (SIR) model show the same absence of epidemic threshold [23]. These results highlight the study of epidemic models in complex networks as potentially relevant also in human and animal epidemiology [23], as confirmed recently by the experimental observation that the web architecture of sexual contacts is best described by a scale-free topology in which individuals have widely different connectivities [24].

In this paper we provide a detailed analytical and numerical study of the SIR model on two prototype complex networks: the Watts-Strogatz (WS) model and the Barabási - Albert (BA) model. The first model is a small-world network with bounded connectivity fluctuations, while the second one is the prototype example of SF network. The analytical approach allows us to recover the total size of the epidemics in an infinite population, in agreement with earlier estimates [23]. We are able to find the analytic expression for the critical threshold as a function of the moments of the connectivity distribution and we confirm the absence of any finite threshold for connectivity distributions  $P(k) \sim k^{-2-\gamma}$  with

$0 < \gamma \leq 3$ . We obtain the general analytic expression for the total density of infected individuals and the epidemic threshold at arbitrary  $\gamma$  values. Finite size network effects can be easily evaluated from the analytic expressions. Time evolution and other effects of heterogeneity such as the relative infection incidence in different connectivity classes can be predicted. In order to confirm the analytical findings we perform large scale numerical simulations on the WS and BA networks. Numerical results are in perfect agreement with the analytical predictions and confirm that the interplay of complex networks topology and epidemic modeling leads to a new and interesting theoretical framework, whose predictions and implications need to be exhaustively explored.

During the completion of this paper we became aware of a preprint by Lloyd and May [25] which reports a comprehensive study of the SIR model in scale free networks. This work extends the preliminary account provided in Ref. [23]

## II. THE SIR MODEL

Our theoretical understanding of epidemic spreading is based on compartmental models, in which the individuals in the population are divided in a discrete set of states [4,26]. In this framework, diseases which result in the immunization or death of infected individuals can be characterized by the classical susceptible-infected-removed (SIR) model [4,26]. In this model individuals can only exist in three different states: susceptible (healthy), infected, or removed (immunized or dead). In a homogeneous system, the SIR model can be described in terms of the densities of susceptible, infected, and removed individuals,  $S(t)$ ,  $\rho(t)$ , and  $R(t)$ , respectively, as a function of time. These three magnitudes are linked through the normalization condition

$$S(t) + \rho(t) + R(t) = 1, \quad (1)$$

and they obey the following system of differential equations:

$$\begin{aligned} \frac{dS}{dt} &= -\lambda \bar{k} \rho S, \\ \frac{d\rho}{dt} &= -\mu \rho + \lambda \bar{k} \rho S, \\ \frac{dR}{dt} &= \mu \rho. \end{aligned} \quad (2)$$

These equations can be interpreted as follows: infected individuals decay into the removed class at a rate  $\mu$ , while susceptibles individual become infected at a rate proportional to both the densities of infected and susceptible individuals. Here,  $\lambda$  is the microscopic spreading (infection) rate, and  $\bar{k}$  is the number of contacts per unit time that is supposed to be constant for the whole population. In writing this last term of the equations we are assuming the *homogeneous mixing* hypothesis [4], which asserts that the force of the infection (the per capita rate of acquisition of the disease by the susceptible individuals) is proportional to the density of infectious individuals. The homogeneous mixing hypothesis is indeed equivalent to a mean-field treatment of the model, in which one assumes that the rate of contacts between infectious and susceptibles is constant, and independent of any possible source of

heterogeneity present in the system. Another implicit assumption of this model is that the time scale of the disease is much smaller than the lifespan of individuals; therefore we do not include in the equations terms accounting for the birth or natural death of individuals.

The most significant prediction of this model is the presence of a nonzero epidemic threshold  $\lambda_c$  [26]. If the value of  $\lambda$  is above  $\lambda_c$ ,  $\lambda > \lambda_c$ , the disease spreads and infects a finite fraction of the population. On the other hand, when  $\lambda$  is below the threshold,  $\lambda < \lambda_c$ , the total number of infected individuals (the epidemic incidence),  $R_\infty = \lim_{t \rightarrow \infty} R(t)$ , is infinitesimally small in the limit of very large populations (the so-called thermodynamic limit [27]). In order to see this point, let us consider the set of equations (2), in which, without lack of generality, we set  $\mu = 1$ . Integrating the equation for  $S(t)$  with the initial conditions  $R(0) = 0$  and  $S(0) \simeq 1$  (i.e., assuming  $\rho(0) \simeq 0$ , a very small initial concentration of infected individuals), we obtain

$$S(t) = e^{-\lambda \bar{k} R(t)}. \quad (3)$$

Combining this result with the normalization condition (1), we observe that the total number of infected individuals  $R_\infty$  fulfills the following self-consistent equation:

$$R_\infty = 1 - e^{-\lambda \bar{k} R_\infty}. \quad (4)$$

While  $R_\infty = 0$  is always a solution of this equation, in order to have a nonzero solution the following condition must be fulfilled:

$$\left. \frac{d}{dR_\infty} (1 - e^{-\lambda \bar{k} R_\infty}) \right|_{R_\infty=0} > 1. \quad (5)$$

This condition is equivalent to the constraint  $\lambda > \lambda_c$ , where the epidemic threshold  $\lambda_c$  takes the value  $\lambda_c = \bar{k}^{-1}$  in this particular case. By using a Taylor expansion at  $\lambda \simeq \lambda_c$  it is then possible to obtain the epidemic incidence behavior  $R_\infty \sim (\lambda - \lambda_c)$  (valid above the epidemic threshold). It is worth remarking that the threshold mechanism is related to the basic reproductive rate  $\mathcal{R}_0 \sim \lambda \bar{k}$  (not to be confused with removed individuals) usually considered by epidemiologist. Only if  $\mathcal{R}_0$  is larger than unity the infection can sustain itself, obviously defining a threshold in the spreading rate  $\lambda$  [28]. As well, in the language of the physics of nonequilibrium phase transition [27], the epidemic threshold can be considered as completely equivalent to a critical point. In analogy with critical phenomena, we can consider  $R_\infty$  as the order parameter of a phase transition and  $\lambda$  as the tuning parameter. In particular, it is easy to recognize that the SIR model is a generalization of the dynamical percolation model, that has been extensively studied in the context of absorbing-state phase transitions [27].

### III. THE SIR MODEL IN COMPLEX NETWORKS

In order to address the effects of contact heterogeneity in epidemic spreading, let us consider the SIR model defined on a network with general connectivity distribution  $P(k)$  and a finite average connectivity  $\langle k \rangle = \sum_k k P(k)$ . Each node of the network represents an individual in its corresponding state (susceptible, infected, or removed), and each link is a

connection along which the infection can spread. The disease transmission on the network is described in an effective way: At each time step, each susceptible node is infected with probability  $\lambda$ , if it is connected to one or more infected nodes. At the same time, each infected individual becomes removed with probability  $\mu$ , that, without lack of generality, we set equal to unity.

In order to take into account the heterogeneity induced by the presence of nodes with different connectivity, we consider the time evolution of the magnitudes  $\rho_k(t)$ ,  $S_k(t)$ , and  $R_k(t)$ , which are the density of infected, susceptible, and removed nodes of connectivity  $k$  at time  $t$ , respectively. These variables are connected by means of the normalization condition

$$\rho_k(t) + S_k(t) + R_k(t) = 1. \quad (6)$$

Global quantities such as the epidemic incidence are therefore expressed by an average over the various connectivity classes; i.e.  $R(t) = \sum_k P(k)R_k(t)$ . At the mean-field level, these densities satisfy the following set of coupled differential equations:

$$\frac{d\rho_k(t)}{dt} = -\rho_k(t) + \lambda k S_k(t) \Theta(t), \quad (7)$$

$$\frac{dS_k(t)}{dt} = -\lambda k S_k(t) \Theta(t), \quad (8)$$

$$\frac{dR_k(t)}{dt} = \rho_k(t). \quad (9)$$

The factor  $\Theta(t)$  represents the probability that any given link points to an infected site. This quantity can be computed in a self-consistent way [18]: The probability that a link points to a node with  $s$  links is proportional to  $sP(s)$ . Thus, the probability that a randomly chosen link points to an infected node is given by

$$\Theta(t) = \frac{\sum_k k P(k) \rho_k(t)}{\sum_s s P(s)} = \frac{\sum_k k P(k) \rho_k(t)}{\langle k \rangle}. \quad (10)$$

In this approximation we are neglecting the connectivity correlations in the network, i.e., the probability that a link points to an infected node is considered independent of the connectivity of the node from which the link is emanating. A more refined approximation would consider the network correlations as given by the conditional probability  $P(k/k')$  that a node with given connectivity  $k'$  is connected to a node with connectivity  $k$  [29]. Nevertheless, as we will see in the next sections, this rather crude approximation is quite able to give account of many of the properties shown by computer simulations of the model.

The equations (7)–(9), combined with the initial conditions  $R_k(0) = 0$ ,  $\rho_k(0) = \rho_k^0$ , and  $S_k(0) = 1 - \rho_k^0$  completely define the SIR model on any complex network with connectivity distribution  $P(k)$ . We will consider in particular the case of a homogeneous initial distribution of infected nodes,  $\rho_k^0 = \rho^0$ . In this case, in the limit  $\rho^0 \rightarrow 0$ , we can substitute  $\rho_k(0) \simeq 0$  and  $S_k(0) \simeq 1$ . Under this approximation, Eq. (8) can be directly integrated, yielding

$$S_k(t) = e^{-\lambda k \phi(t)} \quad (11)$$

where we have defined the auxiliary function

$$\phi(t) = \int_0^t \Theta(t') dt' = \frac{1}{\langle k \rangle} \sum_k k P(k) R_k(t), \quad (12)$$

and in the last equality we have made use of the definition (10). It is worth remarking that the above equations are similar to those obtained in the case of HIV dynamics in heterogeneous populations [3]

In order to get a closed relation for the total density of infected individuals, it results more convenient to focus on the time evolution of the averaged magnitude  $\phi$ . To this purpose, let us compute its time derivative:

$$\frac{d\phi(t)}{dt} = \frac{1}{\langle k \rangle} \sum_k k P(k) \rho_k(t) = \frac{1}{\langle k \rangle} \sum_k k P(k) (1 - R_k(t) - S_k(t)) \quad (13)$$

$$= 1 - \phi(t) - \frac{1}{\langle k \rangle} \sum_k k P(k) S_k(t). \quad (14)$$

Introducing the obtained time dependence of  $S_k(t)$  we are led to the differential equation for  $\phi(t)$

$$\frac{d\phi(t)}{dt} = 1 - \phi(t) - \frac{1}{\langle k \rangle} \sum_k k P(k) e^{-\lambda k \phi(t)}. \quad (15)$$

Once solved Eq. (15), we can obtain the total epidemic incidence  $R_\infty$  as a function of  $\phi_\infty = \lim_{t \rightarrow \infty} \phi(t)$ . Since  $R_k(\infty) = 1 - S_k(\infty)$ , we have

$$R_\infty = \sum_k P(k) (1 - e^{-\lambda k \phi_\infty}). \quad (16)$$

Equations (15) and (16) constitute thus an alternative representation of the model, with respect to Eqs. (7)–(9).

For a general  $P(k)$  distribution, Eq. (15) cannot be solved in a closed form. However, we can still get useful information on the infinite time limit; i.e. at the end of the epidemics. Since we have that  $\rho_k(\infty) = 0$  and consequently  $\lim_{t \rightarrow \infty} d\phi(t)/dt = 0$ , we obtain from Eq. (15) the following self-consistent equation for  $\phi_\infty$

$$\phi_\infty = 1 - \frac{1}{\langle k \rangle} \sum_k k P(k) e^{-\lambda k \phi_\infty}. \quad (17)$$

The value  $\phi_\infty = 0$  is always a solution. In order to have a non-zero solution, the condition

$$\left. \frac{d}{d\phi_\infty} \left( 1 - \frac{1}{\langle k \rangle} \sum_k k P(k) e^{-\lambda k \phi_\infty} \right) \right|_{\phi_\infty=0} > 1 \quad (18)$$

must be fulfilled. This relation implies

$$\frac{1}{\langle k \rangle} \sum_k k P(k) (\lambda k) = \lambda \frac{\langle k^2 \rangle}{\langle k \rangle} > 1. \quad (19)$$

This condition defines the epidemic threshold

$$\lambda_c = \frac{\langle k \rangle}{\langle k^2 \rangle} \quad (20)$$

below which the epidemic incidence is null, and above which it attains a finite value. That is, the threshold is inversely proportional to the connectivity fluctuations  $\langle k^2 \rangle$ . For regular networks, in which  $\langle k^2 \rangle < \infty$ , the threshold has a finite value and we are in the presence of a standard phase transition. On the other hand, networks with strongly fluctuating connectivity distribution, show a *vanishing* epidemic threshold for increasing network sizes; i.e.  $\langle k^2 \rangle \rightarrow \infty$  for  $N \rightarrow \infty$ . The absence of any intrinsic epidemic threshold in this network can be understood by noticing that in heterogeneous systems the basic reproductive number  $\mathcal{R}_0$  contains a correction term linearly dependent on the fluctuations (standard deviation) of the nodes' connectivity distribution [4,23]. In SF networks the divergence of the connectivity fluctuations leads to an  $\mathcal{R}_0$  that always exceeds unity whatever the spreading rate  $\lambda$  is. This ensures that epidemics always have a finite probability to survive indefinitely. It is worth remarking that real networks have always a finite size  $N$  and thus an effective threshold, depending on the magnitude of  $\langle k \rangle$  and  $\langle k^2 \rangle$ , that can be easily calculated as a function of  $N$ . This apparent threshold, however is not an intrinsic quantity and it is extremely small for systems with large enough  $N$ .

#### IV. EXPONENTIALLY DISTRIBUTED NETWORKS: THE WATTS-STROGATZ MODEL

The class of exponential networks refers to random graph models which produce a connectivity distribution  $P(k)$  peaked at an average value  $\langle k \rangle$  and decaying exponentially fast for  $k \gg \langle k \rangle$  and  $k \ll \langle k \rangle$ . Typical examples of such a network are the random graph model [30] and the small-world model of Watts and Strogatz (WS) [31]. The latter has recently been the object of several studies as a good candidate for the modeling of many realistic situations in the context of social and natural networks. In particular, the WS model shows the “small-world” property common in random graphs [6]; i.e., the diameter of the graph—the shortest chain of links connecting any two vertices—increases very slowly, in general logarithmically with the network size [32]. On the other hand, the WS model has also a local structure (clustering property) that is not found in random graphs with finite connectivity [31,32]. The WS graph is defined as follows [31,32]: The starting point is a ring with  $N$  nodes, in which each node is symmetrically connected with its  $2m$  nearest neighbors. Then, for every node each link connected to a clockwise neighbor is rewired to a randomly chosen node with probability  $p$ , and preserved with probability  $1 - p$ . This procedure generates a random graph with a connectivity distributed exponentially for large  $k$  [31,32], and an average connectivity  $\langle k \rangle = 2m$ . The graph has small-world properties and a non-trivial “clustering coefficient”; i.e., neighboring nodes share many common neighbors [31,32]. The richness of this model has stimulated an intense activity aimed at understanding the network's properties upon changing  $p$  and the network size  $N$  [6,15,31–34]. At the same time, the behavior of physical models on WS graphs has been investigated, including epidemiological percolation models [13,15,16] and models with epidemic cycles [17].

In the following we focus on the WS model with  $p = 1$ ; it is worth noticing that even in this extreme case the network retains some memory of the generating procedure. The

network, in fact, is not locally equivalent to a random graph in that each node has at least  $K$  neighbors. In the limit  $p \rightarrow 1$ , the connectivity distribution of the WS network, as defined previously, takes the form [35]

$$P(k) = \frac{m^{k-m}}{(k-m)!} e^{-m} \quad \text{for } k \geq m. \quad (21)$$

This is a Poisson distribution, with finite moments. Defining the *factorial moments* [36]

$$\langle X^r \rangle_f \equiv \langle X(X-1)(X-2) \cdots (X-r+1) \rangle, \quad (22)$$

we have for the distribution (21)

$$\langle (k-m)^r \rangle_f = m^r. \quad (23)$$

In particular, from Eq. (23), the first moments of the connectivity distribution are given by

$$\langle k \rangle = 2m, \quad (24)$$

$$\langle k^2 \rangle = m(1 + 4m), \quad (25)$$

$$\langle k^3 \rangle = m(1 + 6m + 8m^2), \quad (26)$$

and, in general,

$$\langle k^n \rangle \sim (2m)^n, \quad (27)$$

for large  $m$ .

For general regular networks, for which  $\langle k^n \rangle < \infty$  for all values of  $n$ , Eqs. (15) and (16) can be approximately solved in the limit  $\phi(t) \rightarrow 0$ , by expanding the exponentials under the summation signs. Thus, for the case of the total epidemic incidence  $R_\infty$  in Eq. (16),

$$R_\infty \simeq \sum_k P(k) \lambda k \phi_\infty = \langle k \rangle \lambda \phi_\infty. \quad (28)$$

That is,  $R_\infty$  is linearly proportional to  $\phi_\infty$ .

On the other hand, by expanding the exponential in Eq. (15) and keeping the most relevant terms, we yield :

$$\frac{d\phi}{dt} \simeq 1 - \phi - \frac{\sum_k k P(k) (1 - \lambda k \phi + \lambda^2 k^2 \phi^2 / 2)}{\langle k \rangle} = \phi \left( -1 + \lambda \frac{\langle k^2 \rangle}{\langle k \rangle} - \lambda^2 \phi \frac{\langle k^3 \rangle}{2 \langle k \rangle} \right). \quad (29)$$

The resulting previous equation can be exactly solved, to yield

$$\phi(t) = \frac{2(\lambda - \lambda_c)}{\langle k^2 \rangle} \frac{1}{\langle k^3 \rangle \lambda^2 + A e^{-(\lambda - \lambda_c)t/\lambda_c}}, \quad (30)$$

where  $\lambda_c$  is defined as in Eq. (20). That is, for  $\lambda < \lambda_c$ ,  $\phi_\infty \rightarrow 0$ , while from  $\lambda > \lambda_c$ , we recover the well-known mean-field behavior  $\phi_\infty \sim (\lambda - \lambda_c)$ , which translated to the total epidemic incidence  $R_\infty$  yields



$$R_\infty \sim (\lambda - \lambda_c) \quad (31)$$

In the particular case of the WS networks, we expect to observe the behavior dictated by Eq. (31), with an epidemic threshold given by

$$\lambda_c = \frac{\langle k \rangle}{\langle k^2 \rangle} = \frac{2}{1 + 4m}. \quad (32)$$

In order to compare with the analytical predictions we have carried out large scale simulations of the SIR model in the WS network with  $p = 1$ . In our simulations we consider the WS network with parameter  $m = 3$ , which corresponds to an average connectivity  $\langle k \rangle = 6$ . Simulations were implemented on graphs with number of nodes ranging from  $N = 10^3$  to  $N = 3 \times 10^6$ , averaging over at least  $10^4$  different epidemic outbreaks, performed on at least 10 different realization of the random network. In Fig. 1, we show the total density of removed nodes at the end of the epidemic outbreak as a function of the parameter  $\lambda$ . The graph exhibits an epidemic threshold at  $\lambda_c = 0.184(5)$  that is approached with a roughly linear behavior by  $R_\infty$ . A linear fit to the form  $R_\infty \sim (\lambda - \lambda_c)^\beta$  provides an exponent  $\beta = 0.9(1)$ , in reasonable agreement with the analytical finding. This confirms that the SIR model in exponentially bounded complex networks has a behavior similar to that obtained with the homogeneous mixing hypothesis. Actually, since the connectivity fluctuations are very small in the WS graph ( $\langle k^2 \rangle \sim \langle k \rangle$ ), as a first approximation we can consider the WS model as a homogeneous one in which each node has the same number of links,  $k \simeq \langle k \rangle$ . In order to provide further evidence to this effective homogeneity, we show in Fig. 2 the time evolution of the density of infected nodes for epidemic outbreaks starting only on nodes with a given connectivity  $k$ . The total epidemic incidence is almost constant for all connectivity  $k$ , with a slight shift of the peak time of the outbreak. The figure clearly shows that the system reacts almost identically to this heterogeneous initial conditions, confirming that the homogeneity assumption is correctly depicting the system's behavior. We shall see in the next section that this is not the case for SF networks.

## V. POWER-LAW DISTRIBUTED NETWORKS: THE BARABÁSI-ALBERT MODEL

The Barabási-Albert (BA) graph was introduced as a model of growing network (such as the Internet or the world-wide-web) in which the successively added nodes establish links with higher probability pointing to already highly connected nodes [8]. This is a rather intuitive phenomenon on the Internet and other social networks, in which new individuals tend to develop more easily connections with individuals which are already well-known and widely connected. The BA graph is constructed using the following algorithm [8]: We start from a small number  $m_0$  of disconnected nodes; every time step a new vertex is added, with  $m$  links that are connected to an old node  $i$  with probability

$$\Pi(k_i) = \frac{k_i}{\sum_j k_j}, \quad (33)$$

where  $k_i$  is the connectivity of the  $i$ -th node. After iterating this scheme a sufficient number of times, we obtain a network composed by  $N$  nodes with connectivity distribution  $P(k) \sim k^{-3}$

and average connectivity  $\langle k \rangle = 2m$  (in this work we will consider the parameters  $m_0 = 5$  and  $m = 3$ ). Despite the well-defined average connectivity, the scale invariant properties turn out to play a major role on the physical properties of these networks (for instance, the resilience to attack [13,14]).

In the continuous  $k$  approximation, that substitutes the discrete variable  $k$  for a continuous variable in the range  $[m, \infty[$ , the connectivity distribution of the BA model takes the form

$$P(k) = \frac{2m^2}{k^3} \quad \text{for } k \geq m. \quad (34)$$

For this distribution, the first moment is finite,  $\langle k \rangle = 2m$ , but the second moment diverges with the network size,  $\langle k^2 \rangle \sim \log N$ . In view of the general result, Eq. (20), we observe that the epidemic threshold in this particular network tends to zero for large  $N$ . Also, the general solutions obtained in Sec. 4 cannot be applied, and we must work out the particular solutions of Eqs. (16) and (15).

The equation for  $R_\infty$ , with the connectivity distribution (34) is

$$R_\infty = 1 - 2m^2 \int_m^\infty k^{-3} e^{-\lambda k \phi_\infty} dx = 1 - 2z^2 \int_z^\infty x^{-3} e^{-x} dx, \quad (35)$$

where we have defined the new variable  $z = \lambda m \phi$ . Performing the integral, we obtain

$$R_\infty = 1 - e^{-z}(1 - z) - z^2 \Gamma(0, z), \quad (36)$$

where  $\Gamma(a, z)$  is the incomplete Gamma function [37]. For small values of  $z$ , the function  $\Gamma(0, z)$  can be expanded in the expression [37]

$$\Gamma(0, z) \simeq -(\gamma_E + \ln(z)) + z + \mathcal{O}(z^2), \quad (37)$$

where  $\gamma_E$  is the Euler's constant. By inserting this expansion into the expression for  $R_\infty$ , we obtain for small values of  $\phi_\infty$

$$R_\infty \simeq 2z \equiv \lambda \langle k \rangle \phi_\infty. \quad (38)$$

On its turn, the equation for  $\phi(t)$ , with the connectivity distribution (34) is

$$\frac{d\phi(t)}{dt} = 1 - \phi(t) - m \int_m^\infty k^{-2} e^{-\lambda k \phi} dk. \quad (39)$$

Defining the new variable  $z = \lambda m \phi$ , we can rewrite the previous equation as

$$\frac{1}{\lambda m} \frac{dz}{dt} = 1 - \frac{z}{\lambda m} - z \int_z^\infty x^{-2} e^{-x} dx. \quad (40)$$

In order to study the limit  $z(\phi) \rightarrow 0$  we must first integrate by parts the integral in Eq. (40), to get

$$\frac{1}{\lambda m} \frac{dz}{dt} = 1 - \frac{z}{\lambda m} - e^{-z} - z \ln(z) e^{-z} - z \int_z^\infty \ln(x) e^{-x} dx. \quad (41)$$

We can now take the limit  $z \rightarrow 0$  in the last integral, obtaining

$$\int_0^\infty \ln(x) e^{-x} dx = -\gamma_E, \quad (42)$$

where again  $\gamma_E$  is Euler's constant. Introducing this approximation, and Taylor expanding the expression (41), we obtain

$$\frac{1}{\lambda m} \frac{dz}{dt} \simeq z \left[ 1 - \gamma_E - \frac{1}{\lambda m} - \ln(z) \right]. \quad (43)$$

This equation can be integrated, to yield

$$\phi \simeq \frac{1}{\lambda m} \exp \left( 1 - \gamma_E - \frac{1}{\lambda m} - A e^{-\lambda m t} \right), \quad (44)$$

where  $A$  is an integration constant. The stationary regime for long times is

$$\phi_\infty \simeq \frac{e^{1-\gamma_E}}{\lambda m} e^{-1/\lambda m}, \quad (45)$$

and by inserting this result into the expression for the total epidemic incidence we find

$$R_\infty \sim e^{-1/\lambda m}. \quad (46)$$

That is, the function  $R_\infty$  is non-zero for any non-zero value of  $\lambda$ , which is in agreement with the predicted threshold  $\lambda_c = 0$ . This result also recovers the same behavior obtained by considering a diverging connectivity variance in the results reported by May and Anderson for HIV spreading in heterogeneous population [3,23].

The numerical simulations performed on the BA network confirm the picture extracted from the analytic treatment. We consider the SIR model on BA networks of size ranging from  $N = 10^3$  to  $N = 10^6$ , with  $m = 3$  and thus  $\langle k \rangle = 6$ . As predicted by the analytic calculations, Fig. 3 shows that  $R_\infty$  decays with  $\lambda$  as  $R_\infty \sim \exp(-C/\lambda)$ , where  $C$  is a constant. In order to rule out the presence of finite size effects hiding an abrupt transition (the so-called smoothing out of critical points [27]), we have inspected the behavior of the stationary persistence for network sizes varying over three orders of magnitude. The total absence of scaling of  $R_\infty$  and the perfect agreement for any size with the analytically predicted exponential behavior allows us to definitely confirm the absence of any finite epidemic threshold. A closer look at  $R_\infty$  is given in Fig. 4. While Fig. 3 reports the average over  $10^4 - 10^5$  epidemic outbreaks, Fig. 4 reports an illustration of the behavior of the cumulative probability  $P(R_\infty > R)$  of having an outbreak which affects  $R$  individuals in a single realization at  $\lambda = 0.09$ . The figure shows a finite probability of having outbreaks involving a number of individuals of the order of the network size  $N$ . The large plateau corresponds to a gap between large events and small outbreaks that give rise to a zero density of infected individuals in the  $N \rightarrow \infty$  limit. Accordingly to the predictions, the plateau extends proportionally to  $N$  for increasing network sizes.

The large heterogeneity of these networks can be pictorially characterized by inspecting the epidemic evolution in each class of connectivity  $k$ . We know from Eq. (11), that the susceptibles densities  $S_k(t)$  decay much faster in the highly connected classes. In particular,

we have that  $S_k(\infty) \sim \exp(-\lambda k \phi_\infty)$ . In Fig. 5, we report  $S_k(\infty)$  as a function of  $k$  on a semi-logarithmic scale. The plot shows the expected linear relation in  $k$ . Since  $R_k(\infty) = 1 - S_k(\infty)$ , the curves clearly show that the higher is the nodes' connectivity, the higher is the relative incidence of the epidemic outbreak. Classes of nodes with few connections have a small density of removed individuals (total number of infected individuals), while highly connected classes ( $k \gg 100$ ) are almost totally affected by the infection. A further striking evidence of the peculiar behavior of the SF networks is obtained by inspecting epidemic outbreaks starting on nodes with different connectivity  $k$ . While an analytical solution for this case is very troublesome, the numerical investigation presents clear-cut results. In Fig. 6 we present the infection incidence profile for epidemic outbreaks started on sites with different connectivities  $k$ . The population results much weaker (higher number of infected individuals) to epidemics starting on highly connected individuals. This weakness points out that the best protection of these networks can be achieved by targeted immunization programs [4,22].

## VI. GENERALIZED SCALE-FREE NETWORKS

Recently there has been a burst of activity in the modeling of SF complex networks. The recipe of Barabási and Albert [8] has been followed by several variations and generalizations [38–41] and the revamping of previous mathematical works [42]. All these studies propose methods to generate SF networks with variable exponent  $\gamma$ . The analytical treatment presented in the previous section for the SIR model can be easily generalized to SF networks with connectivity distribution with  $\gamma > 0$ . Let us consider a generalized SF network with a normalized connectivity distribution given by

$$P(k) = (1 + \gamma)m^{1+\gamma}k^{-2-\gamma}, \quad (47)$$

where we are approximating the connectivity  $k$  as a continuous variable and assuming  $m$  the minimum connectivity of any node. The average connectivity is thus

$$\langle k \rangle = \int_m^\infty k P(k) dk = \frac{1 + \gamma}{\gamma} m, \quad (48)$$

while the connectivity fluctuations are given by

$$\langle k^2 \rangle = \frac{\gamma + 1}{\gamma - 1} m^2 \quad \text{if } \gamma > 1, \quad (49)$$

$$\langle k^2 \rangle = \infty \quad \text{if } \gamma \leq 1. \quad (50)$$

Thus, according to the general result Eq. (20), the epidemic threshold, as a function of  $\gamma$  is

$$\lambda_c = \frac{\gamma - 1}{\gamma m} \quad \text{if } \gamma > 1, \quad (51)$$

$$\lambda_c = 0 \quad \text{if } \gamma \leq 1. \quad (52)$$

To obtain the explicit expression for  $\phi_\infty$  and  $R_\infty$  we must solve the Eqs. (15) and (16) for the general connectivity distribution (47). While the differential equation (15) cannot

be solved in a closed form for general  $\gamma$ , we can obtain approximation to the steady state value at long times,  $\phi_\infty$ , solving the algebraic equation

$$\phi_\infty = 1 - \frac{1}{\langle k \rangle} \sum_k k P(k) e^{-\lambda k \phi_\infty}. \quad (53)$$

As a function of  $\phi_\infty$ , from Eq. (16), the total epidemic incidence  $R_\infty$  takes the form,

$$1 - R_\infty = (1 + \gamma) m^{1+\gamma} \int_m^\infty dk k^{-2-\gamma} e^{-\lambda k \phi_\infty} = (1 + \gamma) z^{1+\gamma} \int_z^\infty x^{-2-\gamma} e^{-x} dx \quad (54)$$

$$= (1 + \gamma) z^{1+\gamma} \Gamma(-1 - \gamma, z), \quad (55)$$

where we have defined  $z = \lambda k \phi_\infty$  and  $\Gamma(a, z)$  is the incomplete Gamma function [37]. In the limit  $z \rightarrow 0$ , we can perform a Taylor expansion of the incomplete Gamma function, with the form [37]

$$\Gamma(a, z) = \Gamma(a) - \frac{z^a}{a} + z^a \sum_{n=1}^\infty \frac{(-z)^n}{(a+n)n!}, \quad (56)$$

where  $\Gamma(a)$  is the standard Gamma function. This expansion has obviously meaning only for  $a \neq -1, -2, -3, \dots$ . Thus, integer values of  $\gamma$  must be analyzed in a case by case basis. Substituting the last formula into the expression for  $R_\infty$ , we are led to

$$R_\infty = \Gamma(-\gamma) z^{1+\gamma} - (1 + \gamma) \sum_{n=1}^\infty \frac{(-z)^n}{(n - \gamma - 1)n!} \simeq \frac{\gamma + 1}{\gamma} z + \mathcal{O}(z^{1+\gamma}). \quad (57)$$

That is, for any value of  $\gamma > 0$ , the leading behavior of  $R_\infty$  is

$$R_\infty \sim \frac{\gamma + 1}{\gamma} z = \lambda \langle k \rangle \phi_\infty, \quad (58)$$

which is equivalent to the expression found for regular networks in Eq. (28).

In order to find the infinite time limit value  $\phi_\infty$ , we must solve the Eq. (53). Substituting the form of the generalized connectivity distribution (47), we have

$$\phi_\infty = 1 - \gamma m^\gamma \int_m^\infty k^{-1-\gamma} e^{-\lambda \phi_\infty k} dk = 1 - \gamma z^\gamma \int_z^\infty x^{-1-\gamma} e^{-x} dx = 1 - \gamma z^\gamma \Gamma(-\gamma, z) \quad (59)$$

where again  $z = \lambda k \phi_\infty$ . Inserting in this last expression the Taylor expansion for the incomplete Gamma function, we obtain

$$\phi_\infty = z^\gamma \Gamma(1 - \gamma) + \gamma \sum_{n=1}^\infty \frac{(-z)^n}{(n - \gamma)n!} \quad (60)$$

The leading behavior of the r.h.s. of this equation depends on the particular value of  $\gamma$  considered.

(a)  $0 < \gamma < 1$ : In this case, we have

$$\phi_\infty \simeq (\lambda m \phi_\infty)^\gamma \Gamma(1 - \gamma), \quad (61)$$

from which we obtain

$$\phi_\infty \simeq (\lambda m)^{\gamma/(1-\gamma)} \Gamma(1-\gamma)^{1/(1-\gamma)}. \quad (62)$$

Combining this result with Eq. (58), we obtain

$$R_\infty \sim \lambda^{1/(1-\gamma)}. \quad (63)$$

In this range of values of  $\gamma$  we recover the absence of the epidemic threshold, and the associated critical behavior, as we have already shown in Sec. V.

(b)  $1 < \gamma < 2$ : To obtain a nontrivial solution for  $\phi_\infty$ , we must keep the first two terms in the Taylor expansion (60), namely:

$$\phi_\infty \simeq (\lambda m \phi_\infty)^\gamma \Gamma(1-\gamma) + \frac{\gamma}{\gamma-1} \lambda m \phi_\infty. \quad (64)$$

From this equation we find

$$\phi_\infty \simeq \left[ \frac{\gamma}{\Gamma(2-\gamma)} \frac{m}{(\lambda m)^\gamma} \left( \lambda - \frac{\gamma-1}{\gamma m} \right) \right]^{1/(\gamma-1)}, \quad (65)$$

which yields

$$R_\infty \simeq (\lambda - \lambda_c)^{1/(\gamma-1)}, \quad (66)$$

with an epidemic threshold  $\lambda_c$  given by Eq. (51).

(c)  $\gamma > 2$ : The most relevant terms in the expansion of  $\phi_\infty$  are now

$$\phi_\infty \simeq \gamma \frac{\lambda m \phi_\infty}{\gamma-1} - \gamma \frac{(\lambda m \phi_\infty)^2}{\gamma-2}. \quad (67)$$

The relevant expression for  $\phi_\infty$  is

$$\phi_\infty \simeq \frac{\gamma-2}{\gamma-1} \frac{1}{\lambda^2 m} \left( \lambda - \frac{\gamma-1}{\gamma m} \right), \quad (68)$$

that for the epidemic incidence yields the behavior

$$R_\infty \simeq (\lambda - \lambda_c). \quad (69)$$

The threshold  $\lambda_c$  is again given by the general expression (51). In other words, we recover the usual epidemic framework in networks with connectivity distribution that decays faster than  $k$  to the fourth power. Obviously, an exponentially bounded network is included in this last case.

## VII. CONCLUSIONS

The presented results for the SIR model in complex networks confirm the epidemiological picture proposed in previous works. The topology of the network has a great influence in the overall behavior of epidemic spreading. The connectivity fluctuations of the network play a major role by strongly enhancing the infection's incidence. This issue assumes a particular relevance in the case of SF networks that exhibit connectivity fluctuations diverging with the increasing size  $N$  of the web. SF networks are therefore very weak in face of infections presenting an effective epidemic threshold that is vanishing in the limit  $N \rightarrow \infty$ . In the case of the SIR model in an infinite population this corresponds to the absence of any epidemic threshold below which major epidemic outbreaks are impossible. These results strengthen the epidemiological framework for complex networks reported for the SIS model [18,19] and proposed as well for the SIR model [23]. The emerging picture is likely going to stimulate the re-analysis of several concepts of standard epidemiology such as the “core group” or the characteristic number of contacts that appears to be ill-defined in SF networks.

The high heterogeneity of SF networks finds signatures also in the peculiar susceptibility to infections starting on the most connected individuals and the different relative incidence within populations of varying connectivity  $k$ . It is reasonable to expect that these features can point at better protection methods for these networks which appear to have practical realization in many technological and biological systems. In this perspective, the introductions of many elements of realism and a better knowledge of the networks temporal pattern are fundamental ingredients towards a better understanding of the spreading of information and epidemics in a wide range of complex interacting systems.

This work has been partially supported by the European Network Contract No. ERBFM-RXCT980183. RP-S also acknowledges support from the grant CICYT PB97-0693. We thank M.-C. Miguel, R. V. Solé, S. Visintin, and R. Zecchina for helpful comments and discussions. We are grateful to A. L. Lloyd and R. M. May for enlightening suggestions and for pointing out to us some fundamental references.

## REFERENCES

- [1] H. W. Hethcote and J. A. Yorke, *Lect. Notes Biomath.* **56**, 1 (1984).
- [2] R. M. May and R. M. Anderson, *Nature* **326**, 137 (1987).
- [3] R. M. May and R. M. Anderson, *Phil. Trans. R. Soc. Lond. B* **321**, 565 (1988).
- [4] R. M. Anderson and R. M. May, *Infectious diseases in humans* (Oxford University Press, Oxford, 1992).
- [5] S. Strogatz, *Nature* **410**, 268 (2001).
- [6] D. J. Watts, *Small worlds: The dynamics of networks between order and randomness* (Princeton University Press, New Jersey, 1999).
- [7] L. A. N. Amaral, A. Scala, M. Barthélemy, and H. E. Stanley, *Proc. Nat. Acad. Sci.* **97**, 11149 (2000).
- [8] A.-L. Barabási and R. Albert, *Science* **286**, 509 (1999).
- [9] M. Faloutsos, P. Faloutsos, and C. Faloutsos, *ACM SIGCOMM '99, Comput. Commun. Rev.* **29**, 251 (1999).
- [10] G. Caldarelli, R. Marchetti, and L. Pietronero, *Europhys. Lett.* **52**, 386 (2000).
- [11] R. Albert, H. Jeong, and A.-L. Barabási, *Nature* **401**, 130 (1999).
- [12] R. A. Albert, H. Jeong, and A.-L. Barabási, *Nature* **409**, 542 (2000).
- [13] D. S. Callaway, M. E. J. Newman, S. H. Strogatz, and D. J. Watts, *Phys. Rev. Lett.* **85**, 5468 (2000).
- [14] R. Cohen, K. Erez, D. ben-Avraham, and S. Havlin, *Phys. Rev. Lett.* **86**, 3682 (2001).
- [15] M. E. J. Newman and D. J. Watts, *Physical Review E* **60**, 5678 (1999).
- [16] C. Moore and M. E. J. Newman, *Phys. Rev. E* **61**, 5678 (2000).
- [17] G. Abramson and M. Kuperman, *Phys. Rev. Lett.* **86**, 2909 (2001).
- [18] R. Pastor-Satorras and A. Vespignani, *Phys. Rev. Lett.* **86**, 3200 (2001).
- [19] R. Pastor-Satorras and A. Vespignani, *Phys. Rev. E* **63**, 066117 (2001).
- [20] H. W. Hethcote, *Theor. Pop. Biol.* **14**, 338 (1978).
- [21] R. M. May and R. M. Anderson, *Math. Biosci.* **72**, 83 (1984).
- [22] R. Pastor-Satorras and A. Vespignani, e-print cond-mat/0107066 (2001).
- [23] A. L. Lloyd and R. M. May, *Science* **292**, 1316 (2001).
- [24] F. Liljeros *et al.*, *Nature* **411**, 907 (2001).
- [25] A. L. Lloyd and R. M. May, unpublished.
- [26] J. D. Murray, *Mathematical Biology* (Springer Verlag, Berlin, 1993).
- [27] J. Marro and R. Dickman, *Nonequilibrium phase transitions in lattice models* (Cambridge University Press, Cambridge, 1999).
- [28] O. Diekmann and J. Heesterbeek, *Mathematical epidemiology of infectious diseases: model building, analysis and interpretation* (John Wiley & Sons, New York, 2000).
- [29] R. Pastor-Satorras, A. Vázquez, and A. Vespignani, e-print cond-mat/0105161 (2001).
- [30] P. Erdős and P. Rényi, *Publ. Math. Inst. Hung. Acad. Sci.* **5**, 17 (1960).
- [31] D. J. Watts and S. H. Strogatz, *Nature* **393**, 440 (1998).
- [32] A. Barrat and M. Weigt, *Eur. Phys. J. B* **13**, 547 (2000).
- [33] M. Barthélemy and L. A. N. Amaral, *Phys. Rev. Lett.* **82**, 3180 (1999).
- [34] M. Argollo de Menezes, C. Moukarzel, and T. J. P. Penna, *Europhys. Lett.* **50**, 574 (2000).
- [35] A. Barrat and M. Weigt, *Eur. Phys. J. B* **13**, 547 (2000).
- [36] C. W. Gardiner, *Handbook of stochastic methods*, 2nd ed. (Springer, Berlin, 1985).



- [37] M. Abramowitz and I. A. Stegun, *Handbook of mathematical functions*. (Dover, New York, 1972).
- [38] R. Albert and A.-L. Barabási, Phys. Rev. Lett. **85**, 5234 (2000).
- [39] S. N. Dorogovtsev, J. J. F. F. Mendes, and A. N. Samukhin, Phys. Rev. Lett. **85**, 4633 (2000).
- [40] P. L. Krapivsky, S. Redner, and F. Leyvraz, Phys. Rev. Lett. **85**, 4629 (2000).
- [41] B. Tadic, Physica A **293**, 273 (2001).
- [42] H. A. Simon, Biometrika **42**, 425 (1955).

# FIGURES

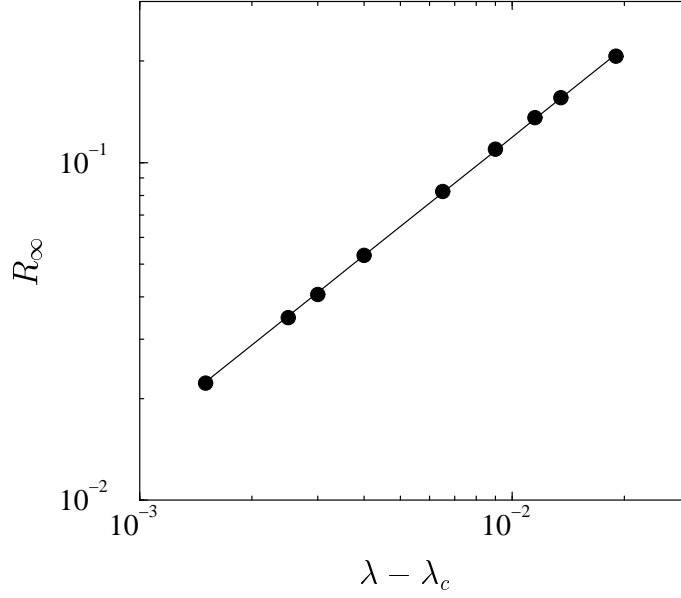


FIG. 1. Total density of infected individuals  $R_\infty$  as a function of  $\lambda - \lambda_c$  for the SIR model in WS networks of size  $N = 10^6$ . The value of  $\lambda_c = 0.184(5)$  is in good agreement with the analytical prediction. The full line is a fit to the form  $R_\infty \sim (\lambda - \lambda_c)^\beta$  with  $\beta = 0.9(1)$ .

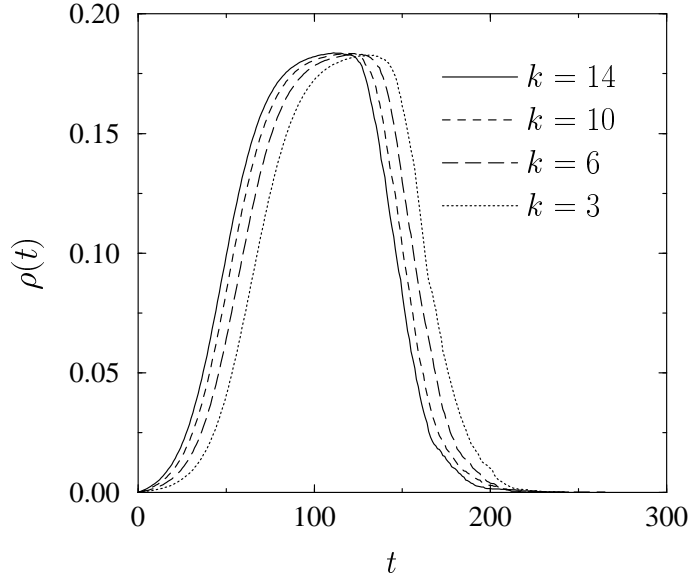


FIG. 2. Total density of infected nodes as a function of time for the SIR model in WS networks, starting from initial conditions peaked in nodes of connectivity  $k$  (initial infected individuals randomly distributed only among the nodes of connectivity  $k$ ). The spreading rate is fixed to  $\lambda = 0.20$ . The network size is  $N = 10^6$ .

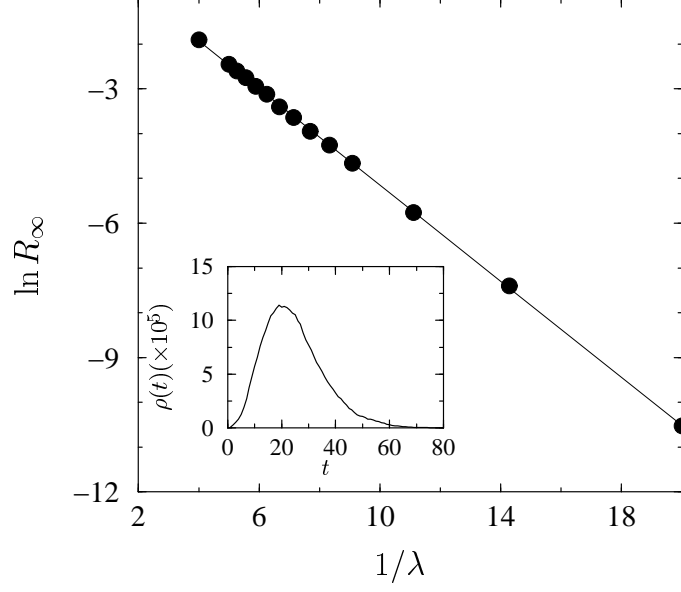


FIG. 3. Total density of infected individuals  $R_\infty$  as a function of  $1/\lambda$  for the SIR model in BA networks of size  $N = 10^6$ . The linear behavior on the semi-logarithmic scale proves the stretched exponential behavior predicted by Eq. (46). The inset show the time profile of the average density of infected individuals at the spreading rate  $\lambda = 0.9$ .

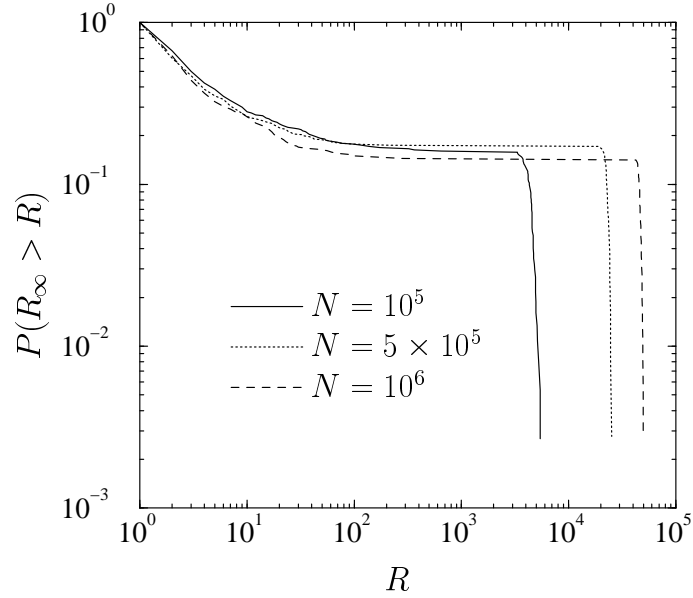


FIG. 4. Cumulated outbreak epidemic distribution for the SIR model in BA networks. The spreading rate is fixed to  $\lambda = 0.09$ .

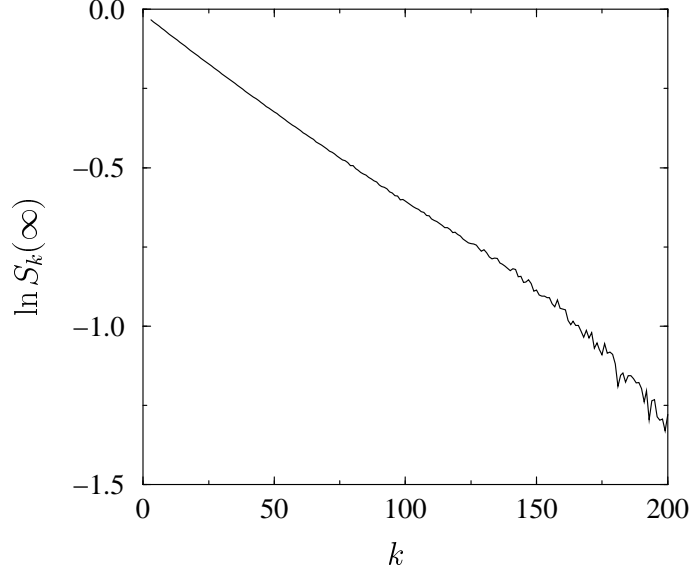


FIG. 5. Density  $S_k(\infty)$  of susceptible nodes as a function of  $k$  for the SIR model in BA networks. Epidemics start from random initial conditions (initial infected individuals randomly distributed among all nodes). The spreading rate is fixed to  $\lambda = 0.09$ . The network size is  $N = 10^6$ . The linear-log plot recovers the exponential form predicted in Eq. (11)

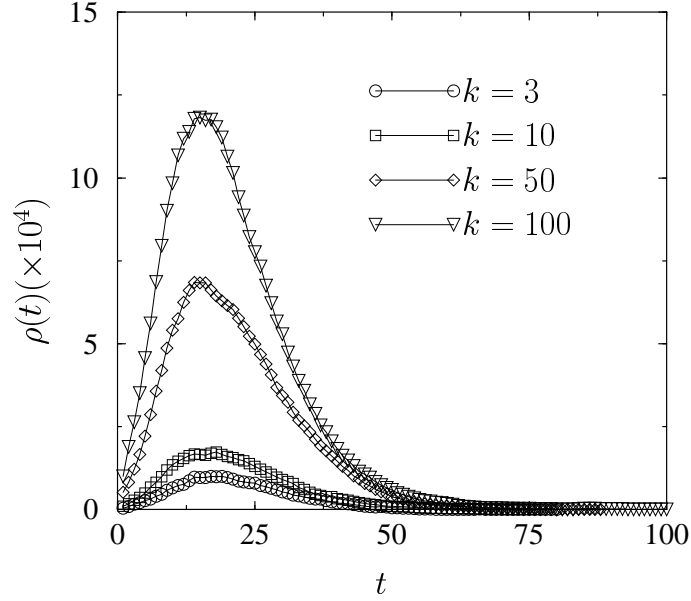


FIG. 6. Total density of infected nodes as a function of time for the SIR model in BA networks, starting from initial conditions concentrated in nodes of connectivity  $k$  (initial infected individuals randomly distributed among the nodes of connectivity  $k$ ). The spreading rate is fixed to  $\lambda = 0.09$ . The network size is  $N = 10^6$ .